Woods Hole Oceanographic Institution

WHOI-94-18

C.1

Technical Report

August 1994

Meteorological and Oceanographic Data Collected during the ASREX 91 Field Experiment

by

Nancy R. Galbraith
Anand Gnanadesikan
George H. Tupper
Bryan S. Way

Upper Ocean Processes Group
Woods Hole Oceanographic Institution

Eugene A. Terray
Department of Applied Ocean Science and Engineering
Woods Hole Oceanographic Institution

Upper Ocean Processes Group
Woods Hole Oceanographic Institution
Woods Hole, Massachusetts 02543

UOP Technical Report 94-1

WHOI-94-18

Meteorological and Oceanographic Data Collected during the ASREX 91 Field Experiment

by

Nancy R. Galbraith
Anand Gnanadesikan
George H. Tupper
Bryan S. Way

Upper Ocean Processes Group
Woods Hole Oceanographic Institution

Eugene A. Terray
Department of Applied Ocean Science and Engineering
Woods Hole Oceanographic Institution

August 1994

Technical Report

Funding was provided by the Ocean Acoustics Program (Code 324OA) of the Office of Naval Research under contract N00014-91-J-1891.

Approved for Distribution:

Philip L. Richardson, Chair
Department of Physical Oceanography

Abstract

The 1991 Acoustic Surface Reverberation Experiment (ASREX 91) took place in November and December off the coast of British Columbia. As part of this experiment, three moorings were deployed to characterize the environmental background. The moorings consisted of a meteorological/oceanographic mooring designed to measure surface meteorology, current and temperature in the upper 120 meters, and nondirectional wave parameters and two wave moorings which were instrumented with pitch-roll buoys to characterize the directional wave spectrum. This report presents results from these three moorings. The conditions seen during the experiment were extremely rough, with wind speeds at 3.4m above the water surface reaching a maximum of 22 m/s and wave heights reaching a maximum of over 10 meters. The air-sea flux of heat was strongly cooling, and the mixed layer deepened over the course of the experiment from approximately 40 to approximately 70 meters. Spectra of the temperature showed a strong semidiurnal tidal signal associated with temperature excursions of several degrees C. The velocity signal showed strong inertial oscillations with amplitudes of 30-50 cm/s Weaker low-frequency and semidiurnal tidal signals were also seen. The waves were very strong with significant wave heights of 5-6 meters persisting for up to 2 weeks at a time. Waves were generally out of the south or the west.

Table of Contents

List of Figures

List of Tables

1. Introduction

The 1991 Acoustic Surface Reverberation Experiment (ASREX 91) was designed to study processes causing degraded acoustic transmission in high sea states. The experiment took place in late 1991 and early 1992 off the coast of British Columbia. In support of this experiment, a group from the Woods Hole Oceanographic Institution deployed three moorings designed to provide the environmental background for the acoustic measurements made by other investigators. These moorings measured the meteorology, temperature structure over the top 120 meters of the water column, current velocity over the top 20 meters, and the directional wave spectrum. The resulting data set provides an opportunity to examine the wintertime deepening of a mixed layer, and to evaluate the importance of surface gravity waves for this process.

2. Mooring Information

The mooring operations took place onboard the University of Washington's *R/V Thomas G. Thompson.* Deployment was on Voyage 4, sailing out of Seattle on 29 October 1991. Recovery was on Voyage 5, also sailing from Seattle, on 5 January 1992. The moorings were sited about 350 km west of Vancouver Island. Table 2.1 lists the location and duration of the three moorings. Figure 2.1 shows a bathymetric map of the area around the experiment site. A list of cruise participants appears in Appendix 1, and the chronology of the cruises is described in Appendix 2.

Table 2.1: Locations and durations of the three moorings

Buoy	Deployment	Recovery	Latitude	Longitude
Discus Buoy (WHOI-920)	911031 21:09	920107 14:18	49 13.45 N	131 51.88 W
Seatex (WHOI-921)	911101 05:50	Surface Buoy 911204 19:00 Mooring: 920107 23:11	49 09.10 N	131 53.30 W
Endeco (WHOI-923)	911102 04:50	920108 18:04	49 08.25 N	131 47.42 W

On 1 December 1991, telemetry data from System Argos revealed that the Seatex buoy had gone adrift. The buoy was recovered on 4 December by the Canadian destroyer *HMCS Huron.* Upon recovery it was found that the Seatex buoy appeared to have been intentionally detached from the mooring and the surface tether had been cut. Information about this incident is given in more detail in Appendix 4.

The WHOI moorings were designed by and set by members of the Upper Ocean Processes Group (UOP) and the Ocean Acoustics Lab (OAL) at Woods Hole. Mooring diagrams are in figures 2.2 through 2.4. A summary of the instrumentation on the discus mooring is given in table 2.2.

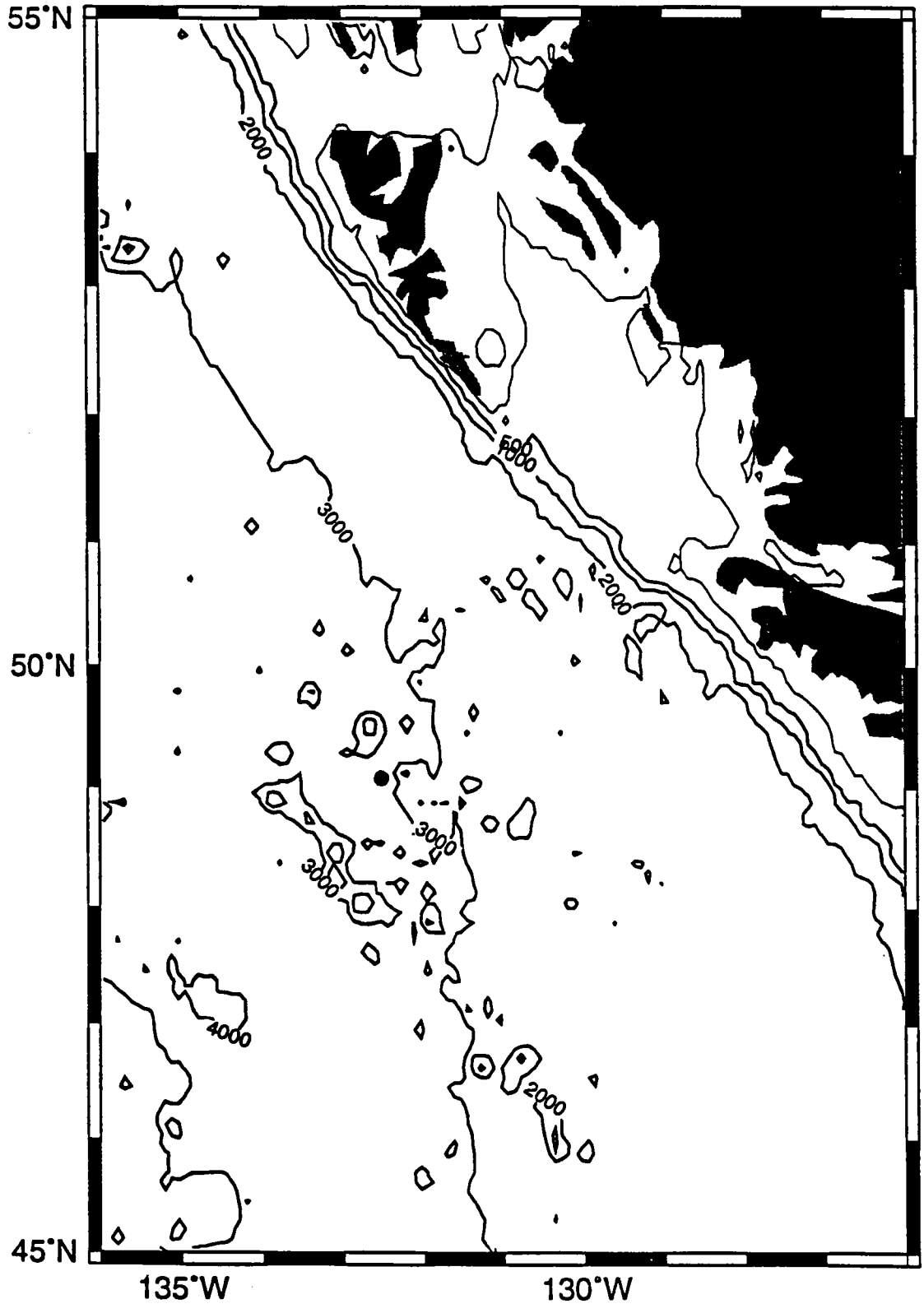

Figure 2.1: Map of ASREX 91 Experiment Site

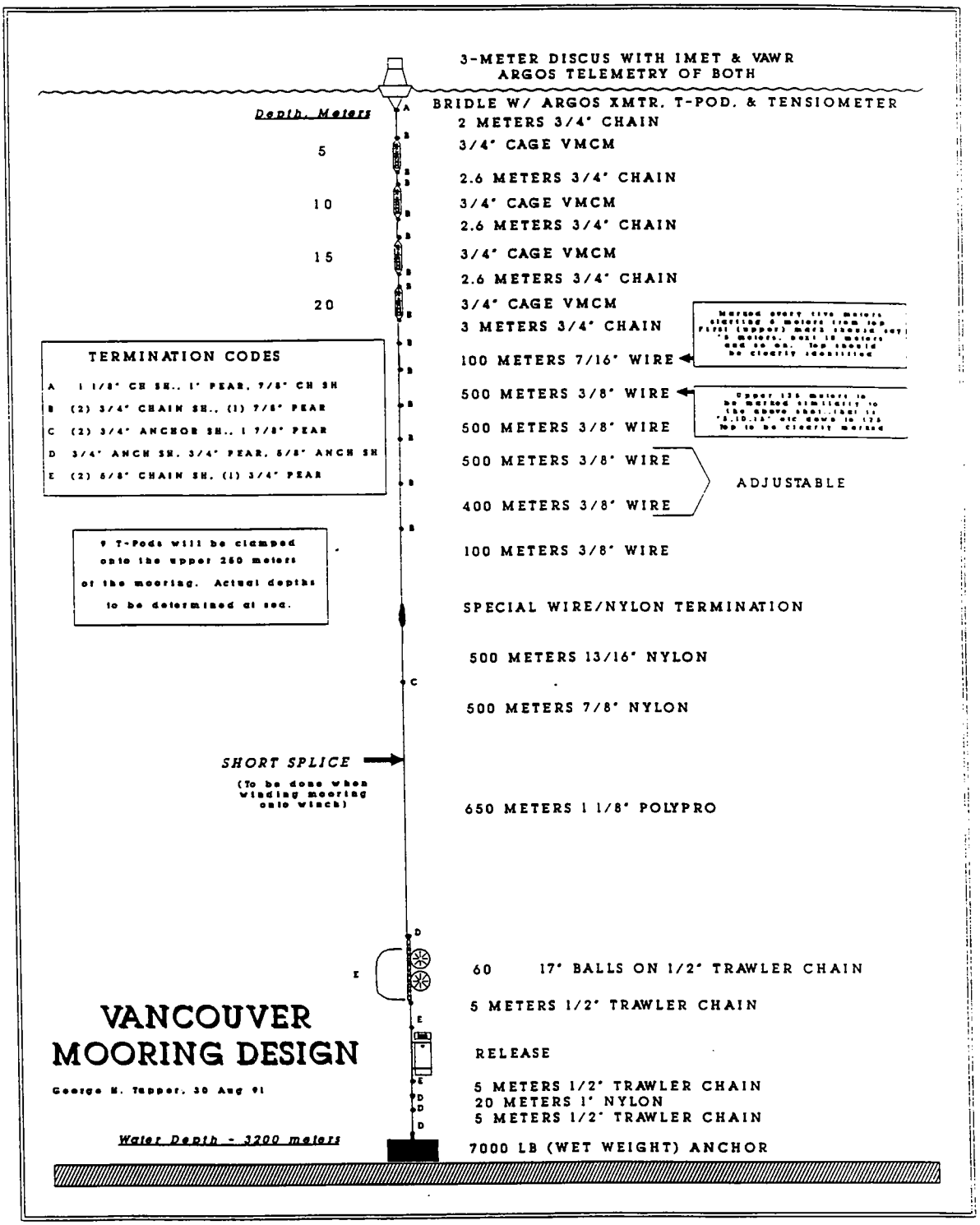

Figure 2.2: Mooring Diagram. Discus Mooring.

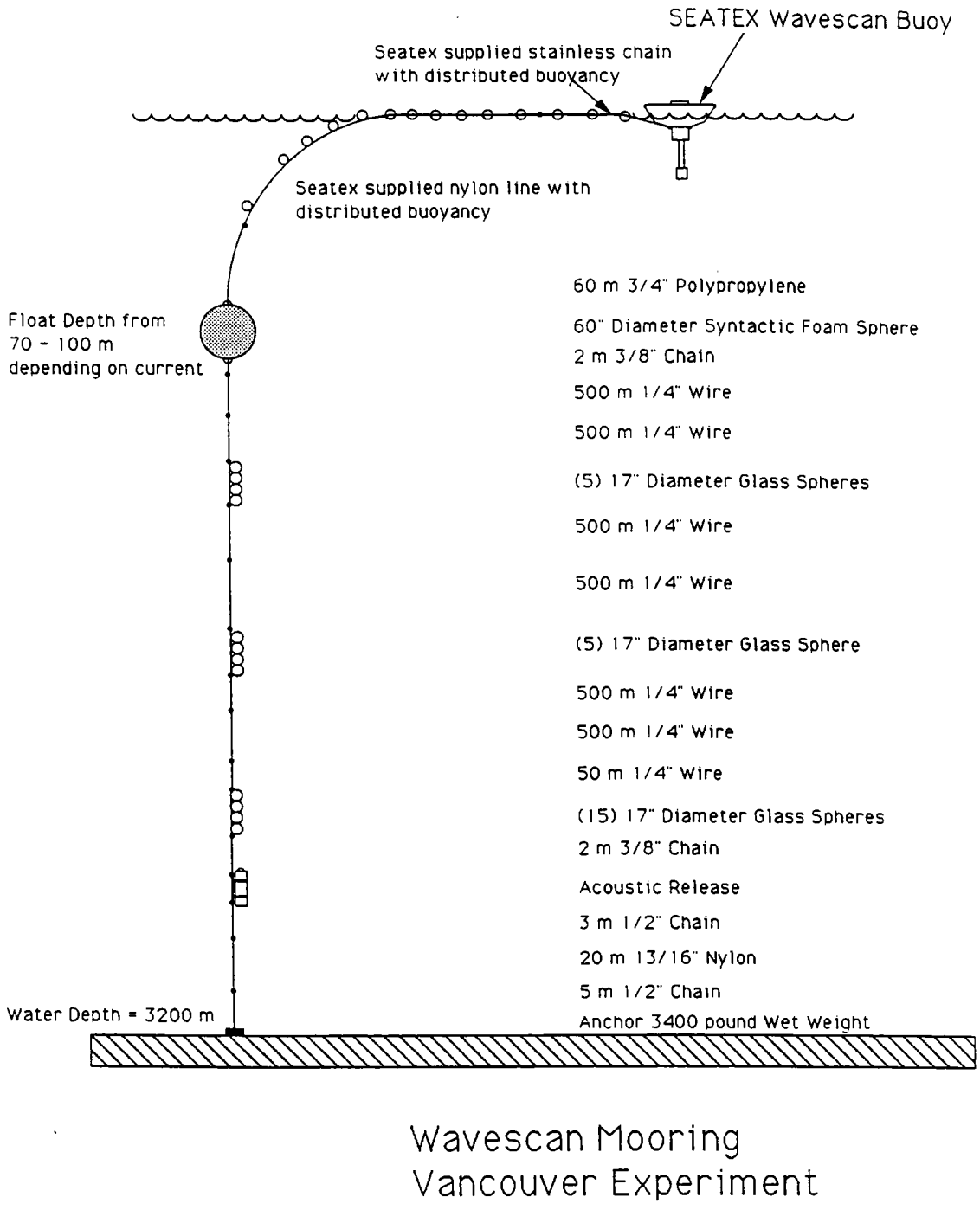

Figure 2.3: Mooring Diagram. Seatex Mooring.

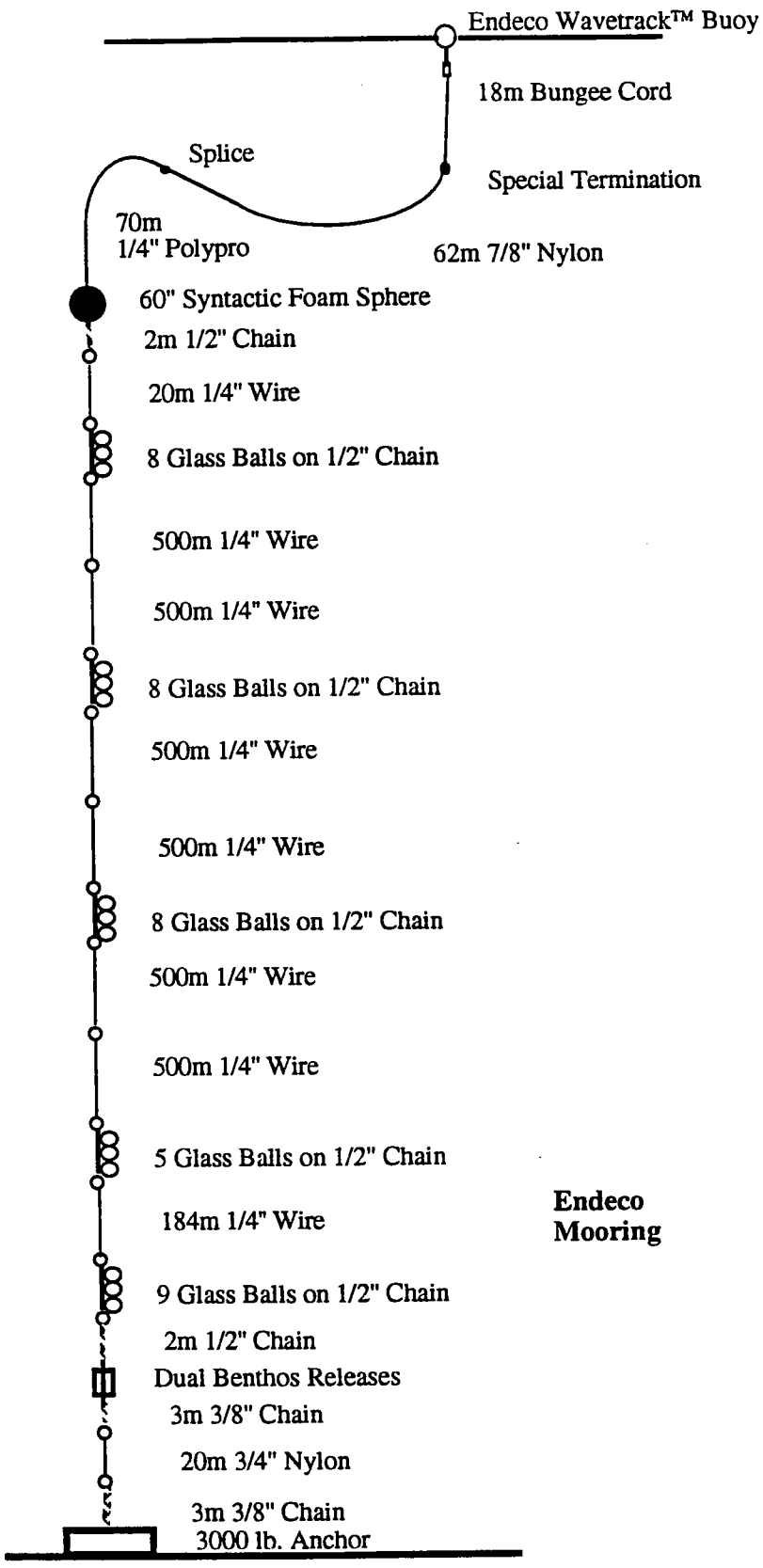

Figure 2.4: Mooring Diagram. Endeco Mooring.

Table 2.2: Instrumentation on the Discus mooring

Instrument Type	Serial Number	Sample Rate(sec)	Depth (meters)
VAWR	0723	900	Surface
IMET		60	Surface
TPOD	3699	450	2
VMCM	1405	112.5	5
VMCM	0201	1125	10
VMCM	0773	112.5	15
VMCM	0873	1125	20
TPOD	3702	450	40
TPOD	3662	450	60
TPOD	3700	450	80
TPOD	3667	450	100
TPOD	3705	450	120

3. Data Presentation

3.1 Meteorology during ASREX 91

Meteorological Observations

Meteorological data was recorded using a Vector-Averaging Wind Recorder (VAWR) with a 15 minute record rate. A second meteorological instrument package, an Improved Meteorological (IMET) system, also recorded data for a period of about one month, but its battery power, normally recharged by solar panels, failed as a result of too little sunlight on 5 December 1991 at midnight. The IMET system had a one minute record rate.

Tables 3.1.1-3.1.2 summarize the sensors, their accuracy, and the sampling strategy for each of the packages. Table 3.1.3 shows a schematic of how the VAWR sampled each sensor during the 15 minute recording interval. Note that while the wind and radiation sensors recorded over the entire interval, the relative humidity and barometric pressure are sampled for a very short period of time in the middle of the recording interval.

A check of the time base for the VAWR found 392 missing or incorrect clock counts. The data was interpolated over these gaps. The final processed data file had a total of 6455 records at 15 minute intervals between 91-11-01 00:07:30 UTC and 92-01-07 08:07:30 UTC. Figure 3.1.1 through 3.1.5 show time-series of meteorological data recorded by the VAWR and IMET. Displayed are wind velocity north and east, sea temperature, air temperature, barometric pressure, relative humidity, short wave and long wave radiation. IMET data is represented with a dashed line, and VAWR data with a solid line. A magnetic variation of 21.4° was applied to the data from both instruments.

The IMET data were found to agree very well with the VAWR data in general, although several small, systematic differences were found. The VAWR recorded wind speeds about 9% higher than the IMET. The IMET relative humidity was found to be about 1% higher than the VAWR with rms differences of order 1-2%. The barometric pressure also showed a systematic offset, with the VAWR being about 0.8 MB lower than the IMET. Except for the wind sensors, these differences were within the sensor specifications. Comparison of these differences with meteorological observations taken aboard the *Thompson* was made, but the differences were not resolvable. For purposes of the flux calculations reported here, the VAWR data will be taken as correct.

Air-Sea Fluxes

Fluxes of momentum, sensible heat, and latent heat for the Vancouver data site were computed from the meteorological variables using the stability-dependent bulk aerodynamic formulae of Large and Pond (1981; 1982). The net shortwave radiation is computed using an albedo of 0.06. The net longwave radiation is estimated using sea surface temperature. air temperature and the mixing ratio from Clark et al., 1974. This formula also includes a cloud-correction function which depends on the cloud cover. The cloud cover n was estimated from the incoming shortwave radiation. by comparing the observed radiation to clear-sky radiation predicted from astronomical theory (List,1984) assuming some atmospheric transmission coefficient. An atmospheric transmission coefficient of 0.7 was used, and compared well with observed short wave radiation from the VAWR during the few clear-sky days over the course of the deployment. Night-

time values of cloud cover were estimated by linear interpolation between the nearest two daytime values.

Time series of the heat fluxes computed from the VAWR are shown in Figures 3.1.6 through 3.1.10. From top to bottom, the sensible, latent, net shortwave, net long wave and total heat flux in W/m^2 are shown. Figures 3.1.11 through 3.1.15 show the wind stress time series computed from the VAWR. From top to bottom, the eastward wind stress, northward wind stress, wind stress magnitude, wind stress direction (towards), and the nondimensional stability parameter z/L . L is the Monin-Obhukhov length $-c_pTu_*^3/\kappa gQ$, (where c_p is the specific heat, T is the temperature , u* the friction velocity, g is gravity, κ is the Von Karman constant, and Q is the heat gained by the atmosphere from the ocean) are shown. Large negative values of L mean that the atmospheric boundary layer is convectively unstable, so that the shear of the velocity is reduced from a logarithmic profile.

Figure 3.1.16 shows the rotary spectrum of the wind stress (solid represents clockwise rotation, dashed counterclockwise rotation), and the spectrum of the sea-surface temperature, air temperature, shortwave radiation, barometric pressure and relative humidity. Other than the shortwave radiation, which shows a distinct set of peaks at the first, second, and third harmonics of the diurnal frequency, there are no significant peaks.

Figure 3.1.17 shows the precipitation measured by the IMET system. The sensor used was an R.M Young self siphoning rain gauge, which emptied itself upon reaching a level of 5 cm. Over the course of the deployment, the gauge emptied itself 2 times, on 3 November and 16 November.

Parameter	Sensor Type	Accuracy	Record Time
Wind Speed	R.M. Young 3-cup Anemometer	+/- 2% above 0.7 m/s	Vector Averaged
Wind Direction	Integral Vane w/vane follower WHOI/EG&G	+/- 1 bit 5.6 degrees	Vector Averaged
Insolation	Pyranometer Eppley 8-48	+/- 3% of reading	Averaged over record interval
Long Wave Radiation	Pyrgeometer Eppley PIR	+/- 10%	Averaged over record interval
Relative Humidity	Vaisala Humicap 0062HMP	+/- 2% RH	3.515 Seconds Average Note 1
Barometric Pressure	Paroscientific Model 216-B-101	+/- 0.2 mbars wind < 20 m/s	2.636 Seconds Average Note 1
Sea Temperature	Thermistor Thermometrics 4K @ 25 degrees C	+/- 0.005 degrees C	Averaged over 1/2 record time Note 2
Air Temperature	Thermistor Yellow Springs #44034 5K @ 25 degrees C	+/- 0.2 degrees C wind > 5 m/s	Averaged over 1/2 record time Note 3

Notes:

1. Relative Humidity and Barometric Pressure are averaged in the middle of the recording interval for the time noted.
2. Sea temperature is measured during the first half of the recording interval.
3. Air temperature is measured during the second half of the recording interval.

Table 3.1.1: Meteorological Sensor Specifications. Vector Averaging Wind Recorder (VAWR) Deployed on Discus Buoy.

IMET (Improved Meteorological Record) (60 second record interval)

Parameter	**Sensor Type**	**Accuracy**	**Record Time**
Wind Speed	R. M. Young propeller Anemometer	± 2% above 0.7 m/s	Scalar average over 1 min
Wind Direction	9 bit encoder KVH compass	± 1 bit 0.7 degrees	Scalar average over 1 min
Insolation	Pyranometer Eppley PSP	± 3% of reading	Averaged over record interval
Long Wave Radiation	Pyrgeometer Eppley PIR	± 10%	Averaged over record interval
Relative Humidity	Rotronics MP-100F	± 2% RH	Averaged over record interval
Barometric Pressure	Air DB1-A	± 0.2 mbars wind < 20 m/s	Averaged over record interval
Sea Temperature	PRT 1k	± 0.005 degrees C	Averaged over record interval
Air Temperature	PRT 1k	± .005 degrees C wind > 5 m/s	Averaged over record interval

Table 3.1.2: Meteorological Sensor Specifications. Improved Meteorological system (IMET) Deployed on Discus Buoy.

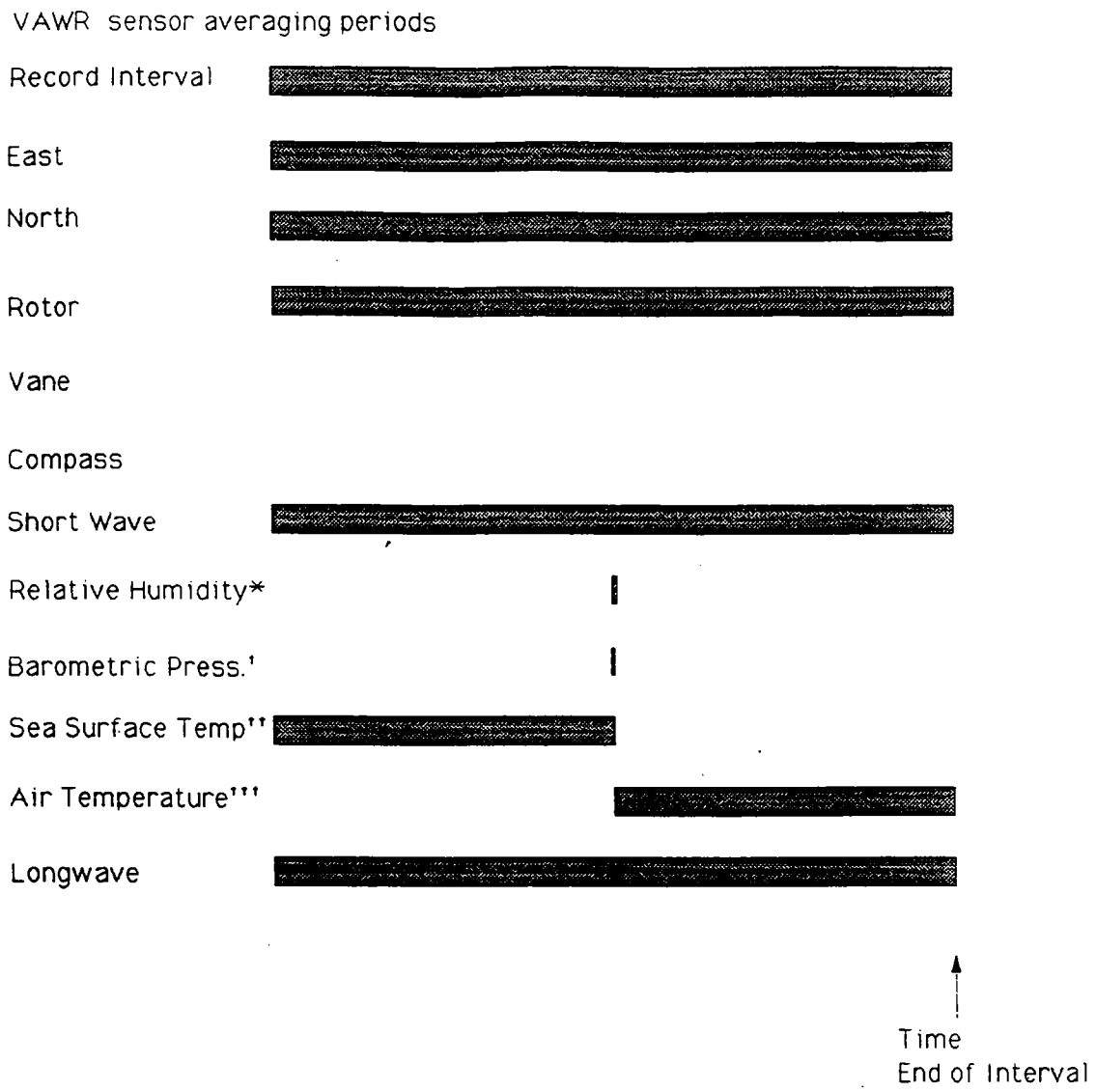

* Relative humidity sensor is on for 7 seconds and counted for 3.515 seconds

' Barometric Pressure sensor is on for 4.39 seconds and counts for 2.636 seconds

'' Sea surface temperature is averaged during the first half of the record rate. Actual averaging interval is half the record rate minus 1.7578125 seconds (delay and settle time from SST to AT)

''' Air temperature is counted for the second half of the averaging interval. The air temp average interval is half the record rate minus 1.7578125.

Recorded compass and vane information is the last sample taken in the record interval.

Table 3.1.3: Schematic of VAWR Sensor Averaging Periods.

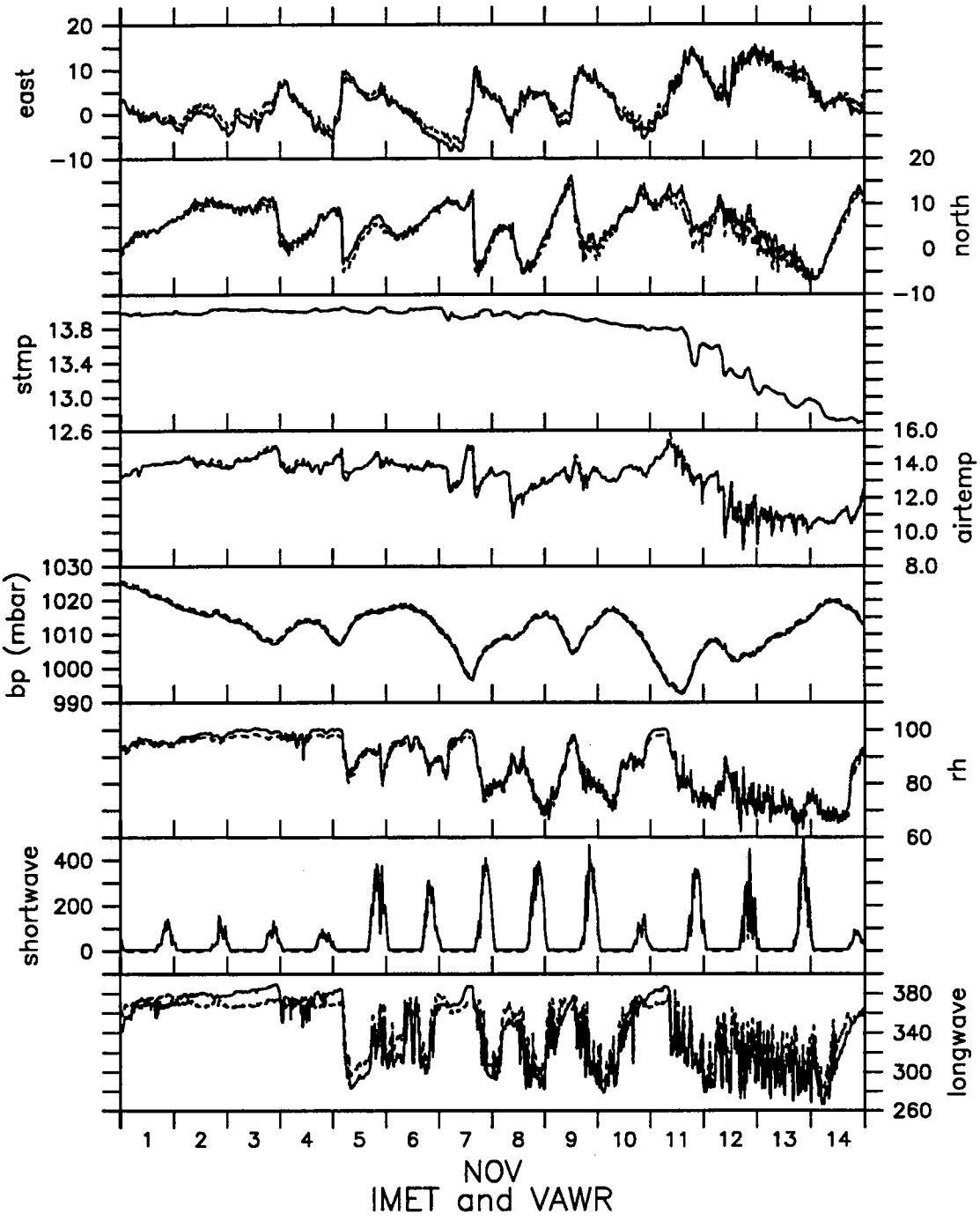

Figure 3.1.1 VAWR and IMET Meteorological Time Series. IMET data is dashed, VAWR data is solid line.

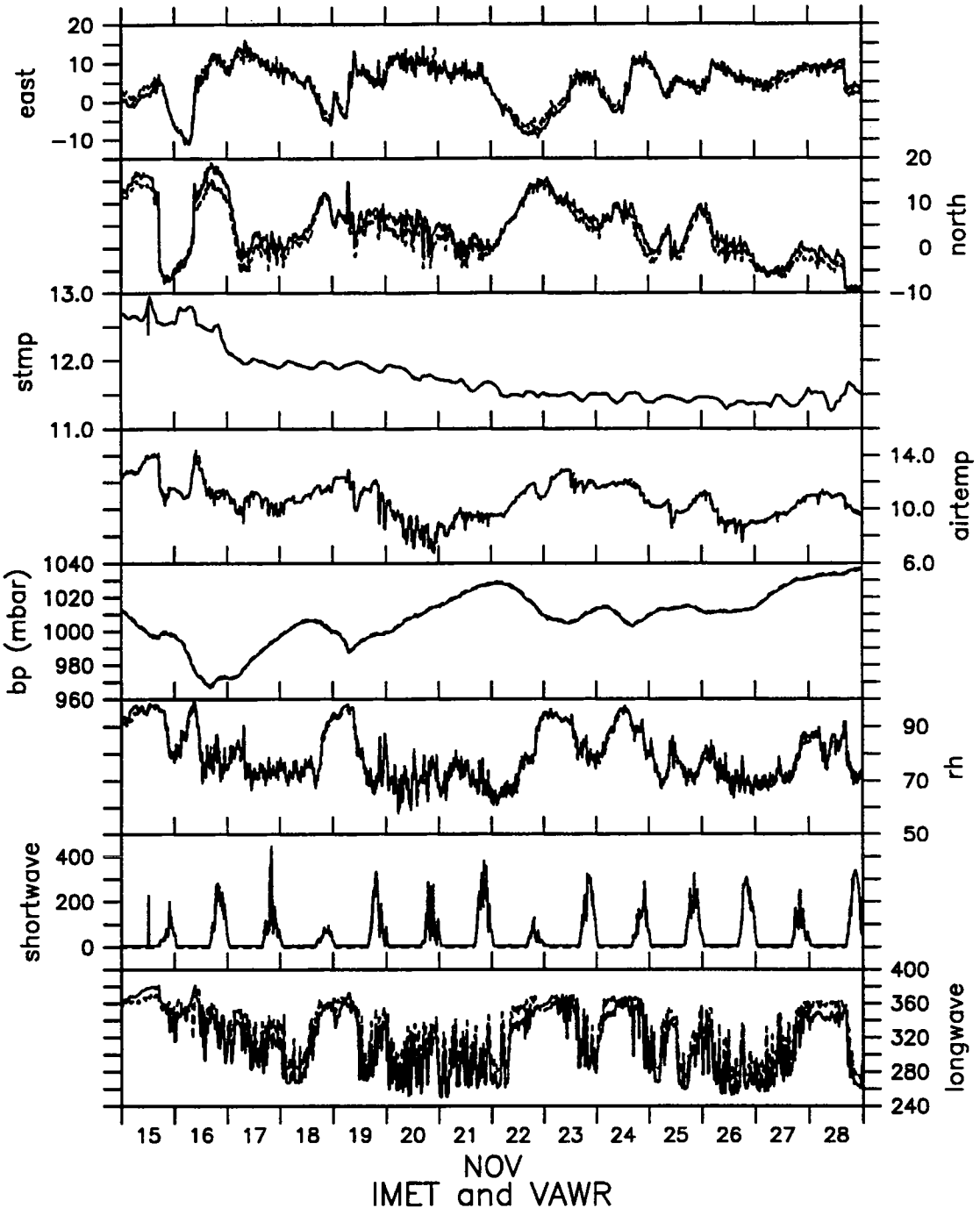

Figure 3.1.2 VAWR and IMET Meteorological Time Series. IMET data is dashed, VAWR data is solid line.

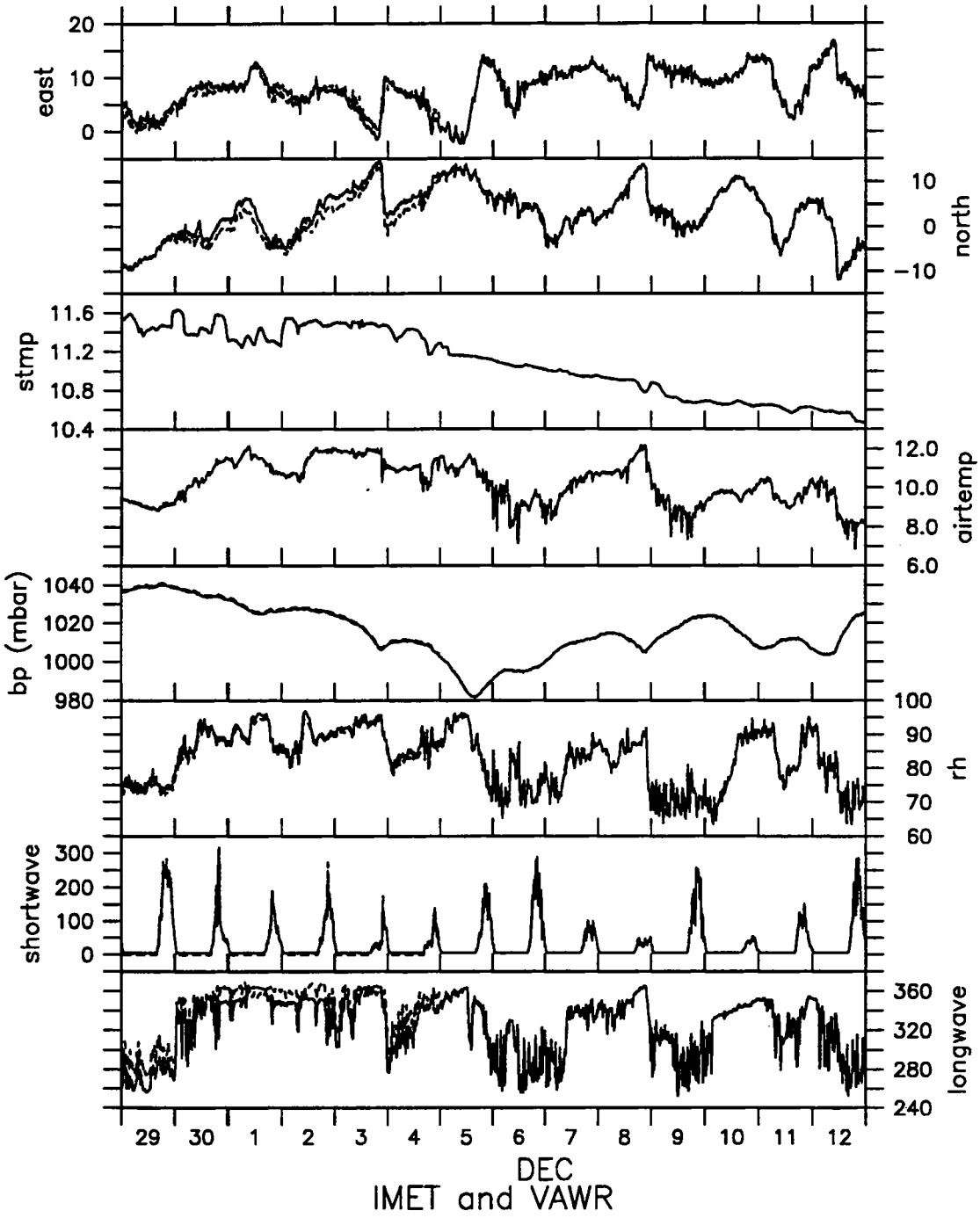

Figure 3.1.3 VAWR and IMET Meteorological Time Series. IMET data is dashed, VAWR data is solid line. IMET failed on December 4 at 2359 UTC.

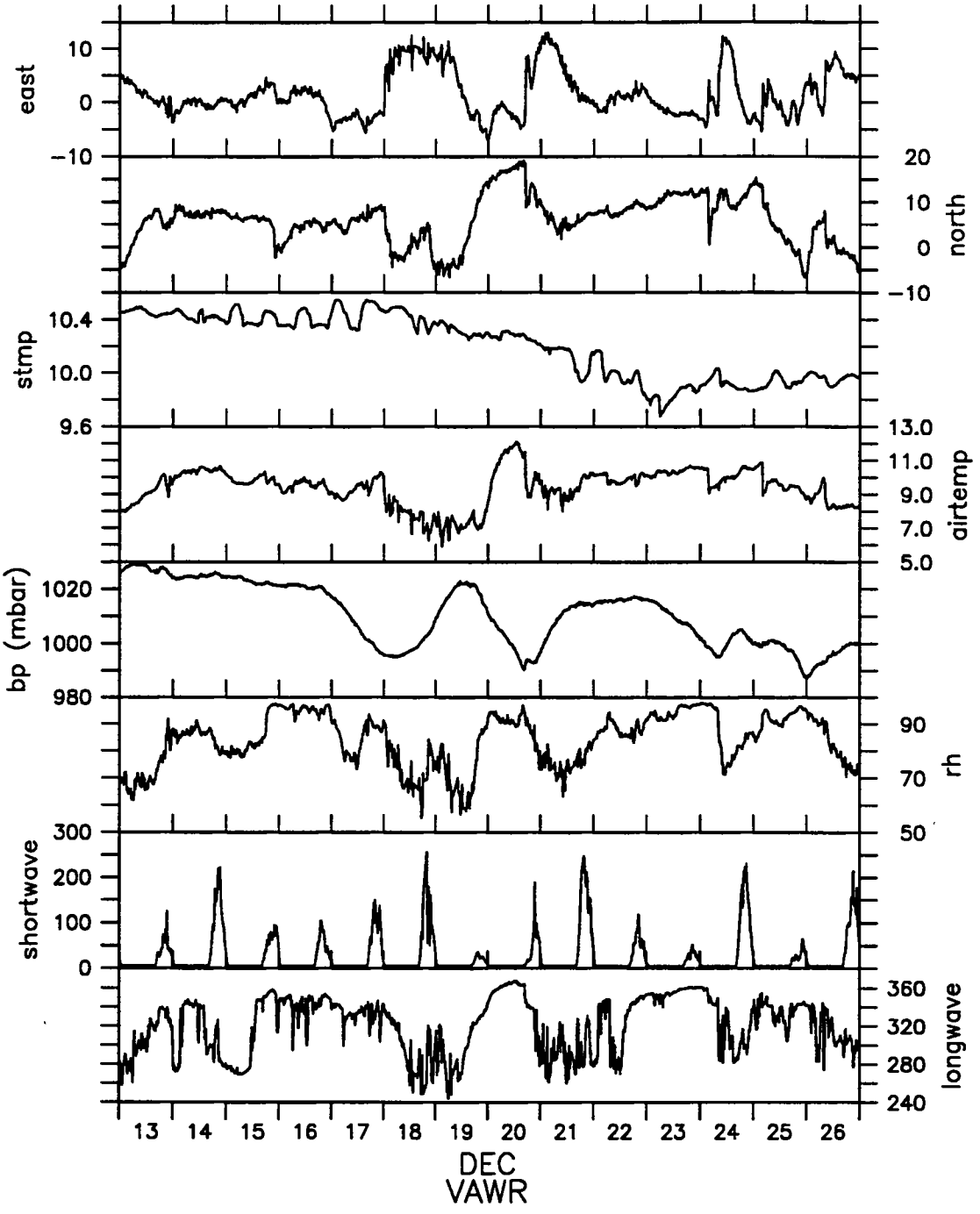

Figure 3.1.4 VAWR Meteorological Time Series.

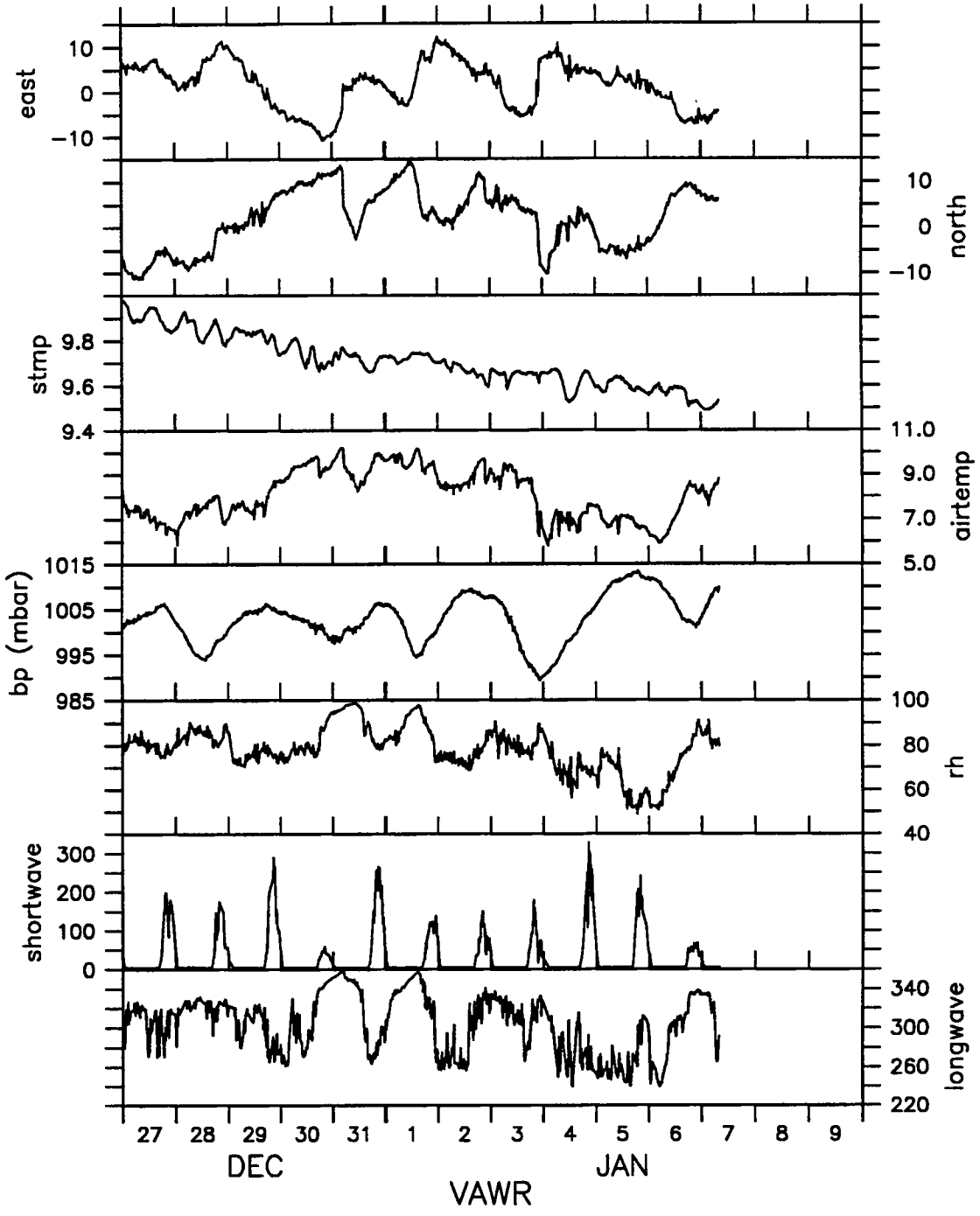

Figure 3.1.5 VAWR Meteorological Time Series.

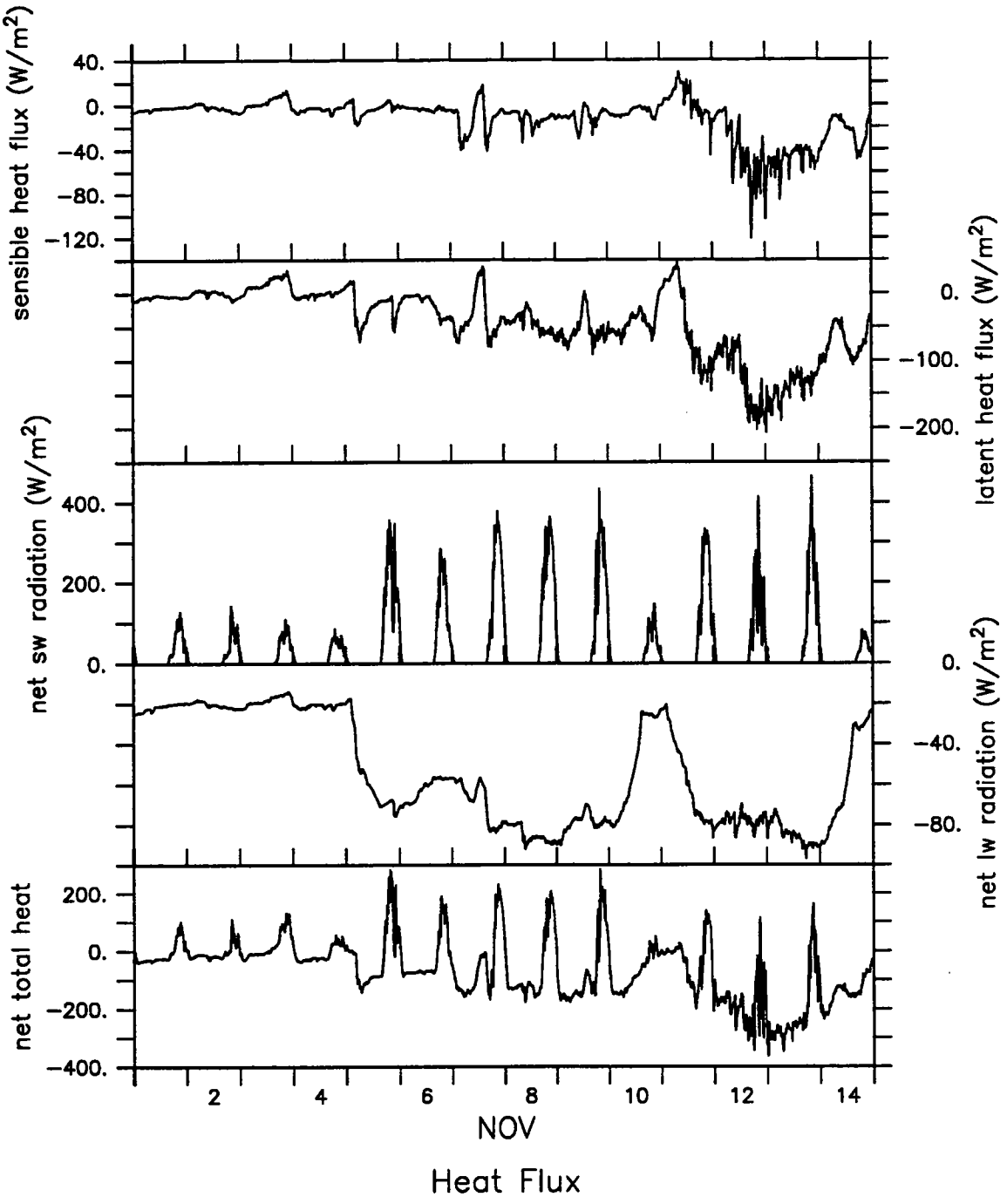

Figure 3.1.6 Heat Flux Time Series from VAWR.

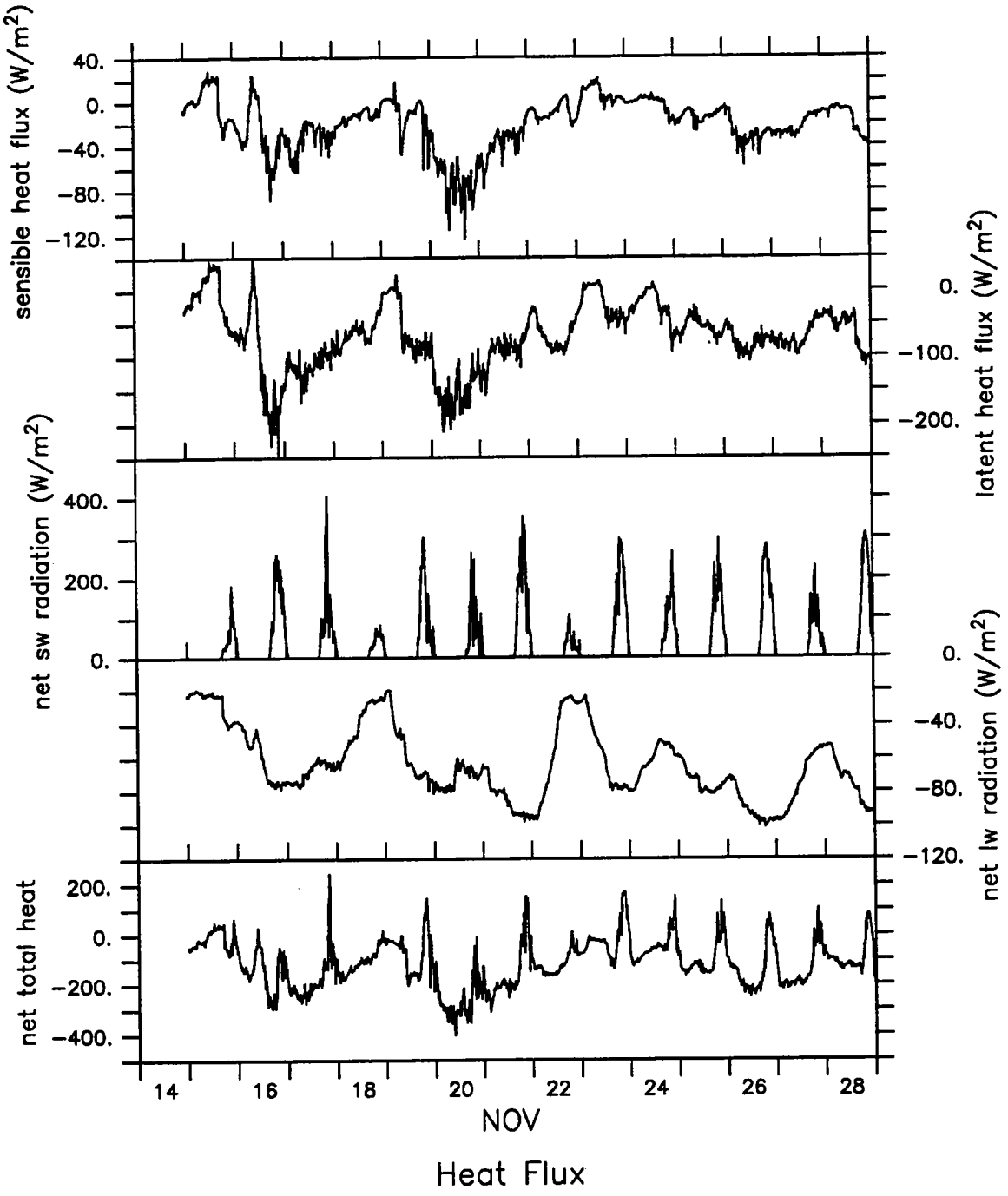

Figure 3.1.7 Heat Flux Time Series from VAWR.

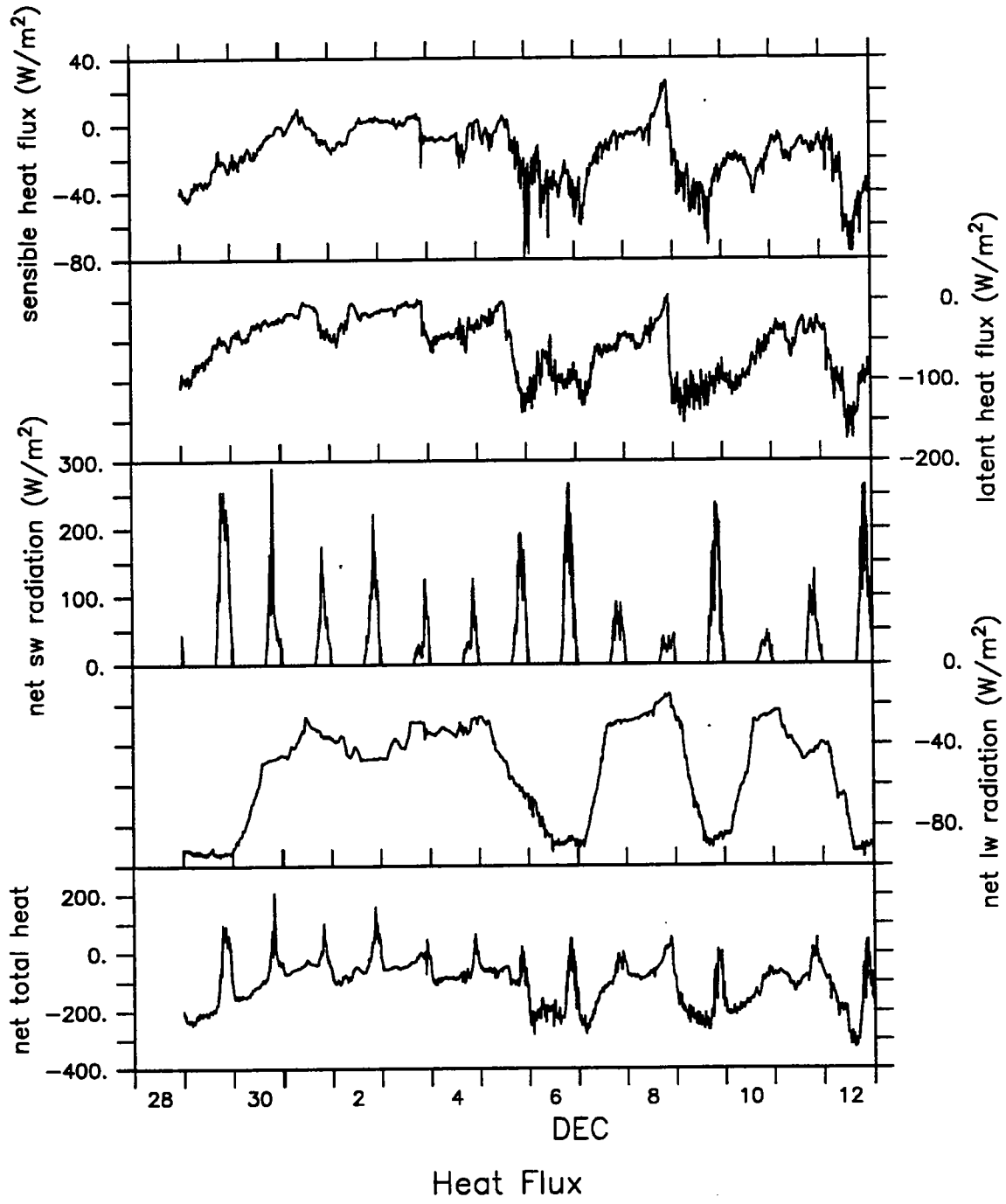

Figure 3.1.8 Heat Flux Time Series from VAWR.

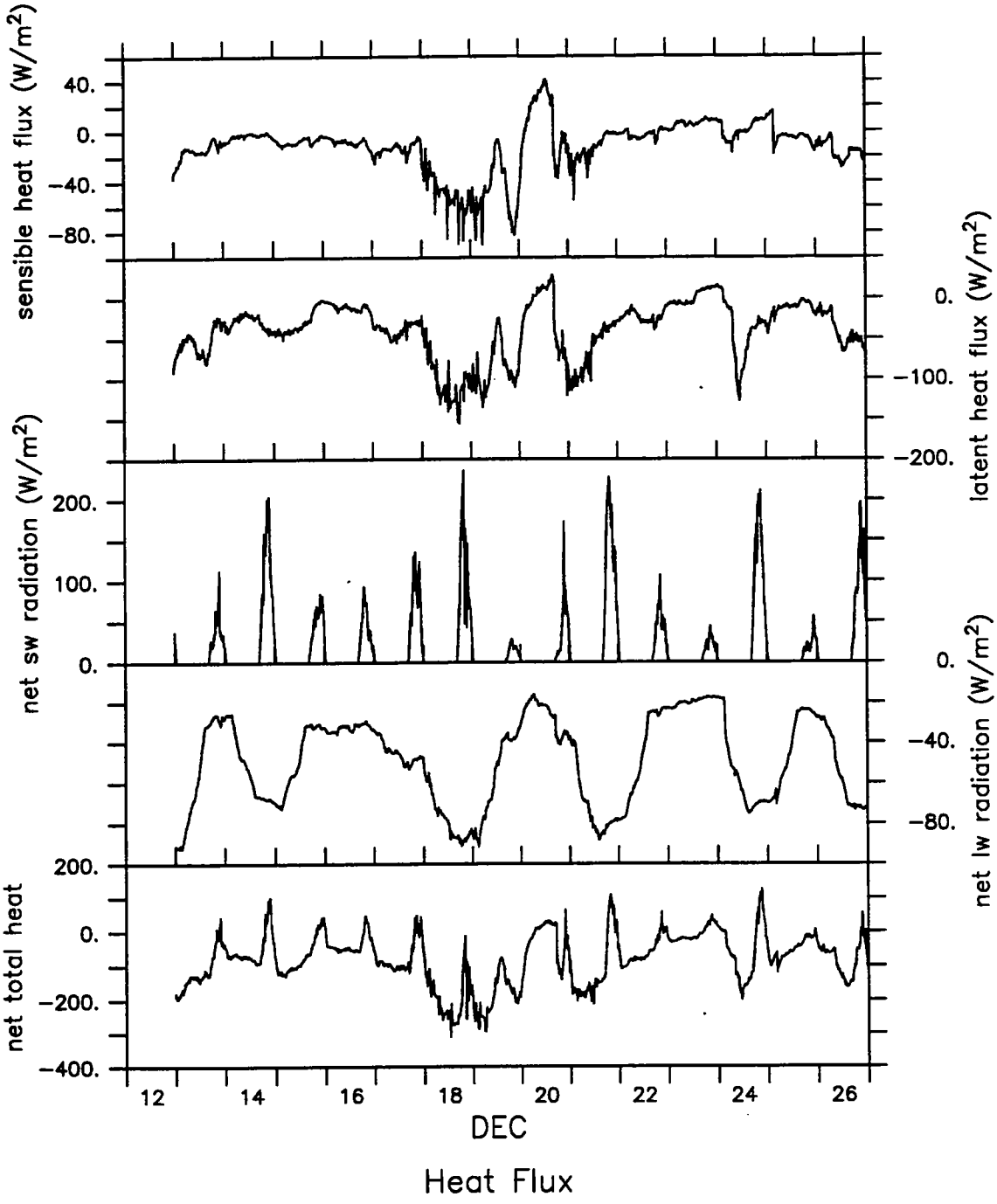

Figure 3.1.9 Heat Flux Time Series from VAWR.

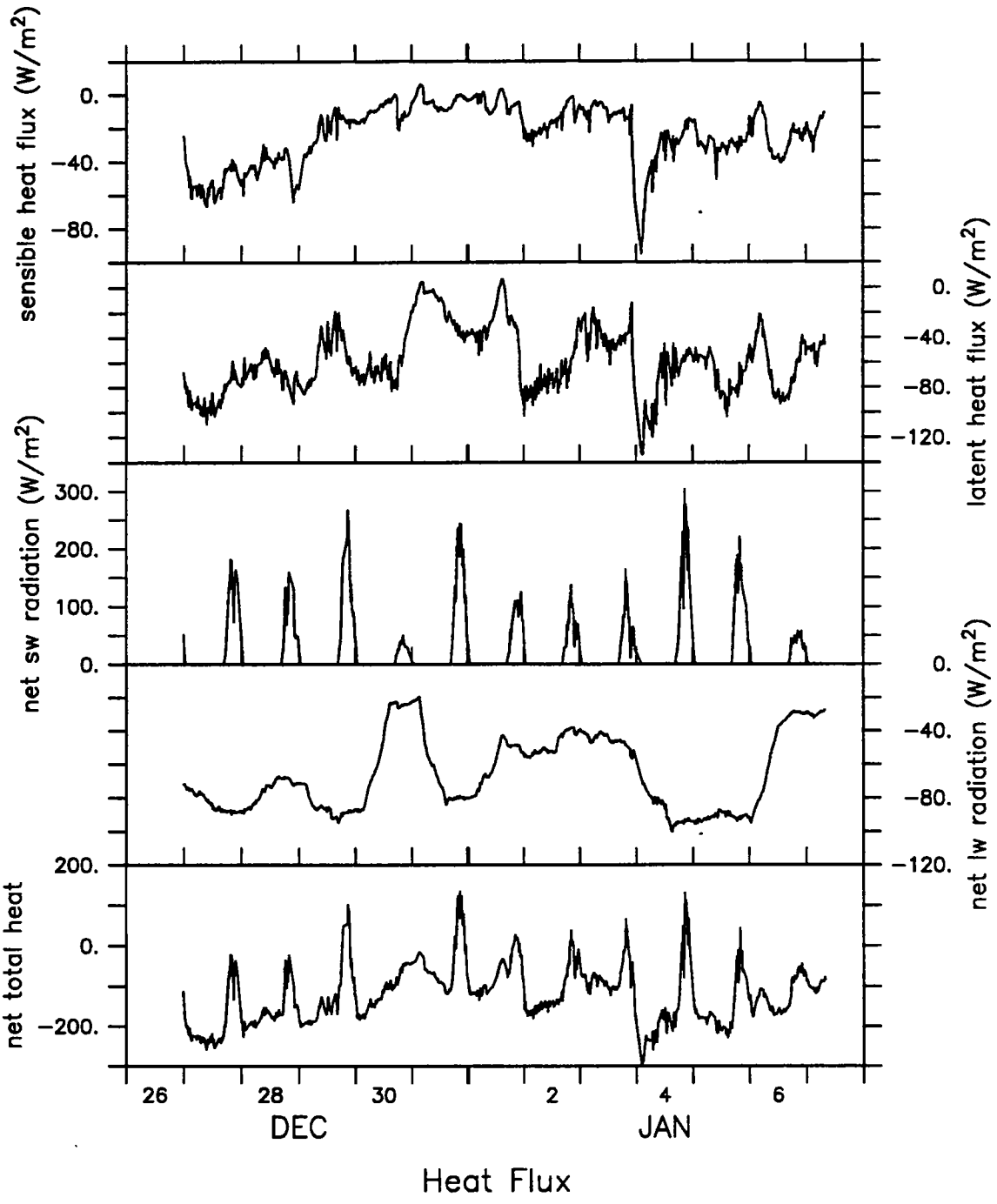

Figure 3.1.10 Heat Flux Time Series from VAWR.

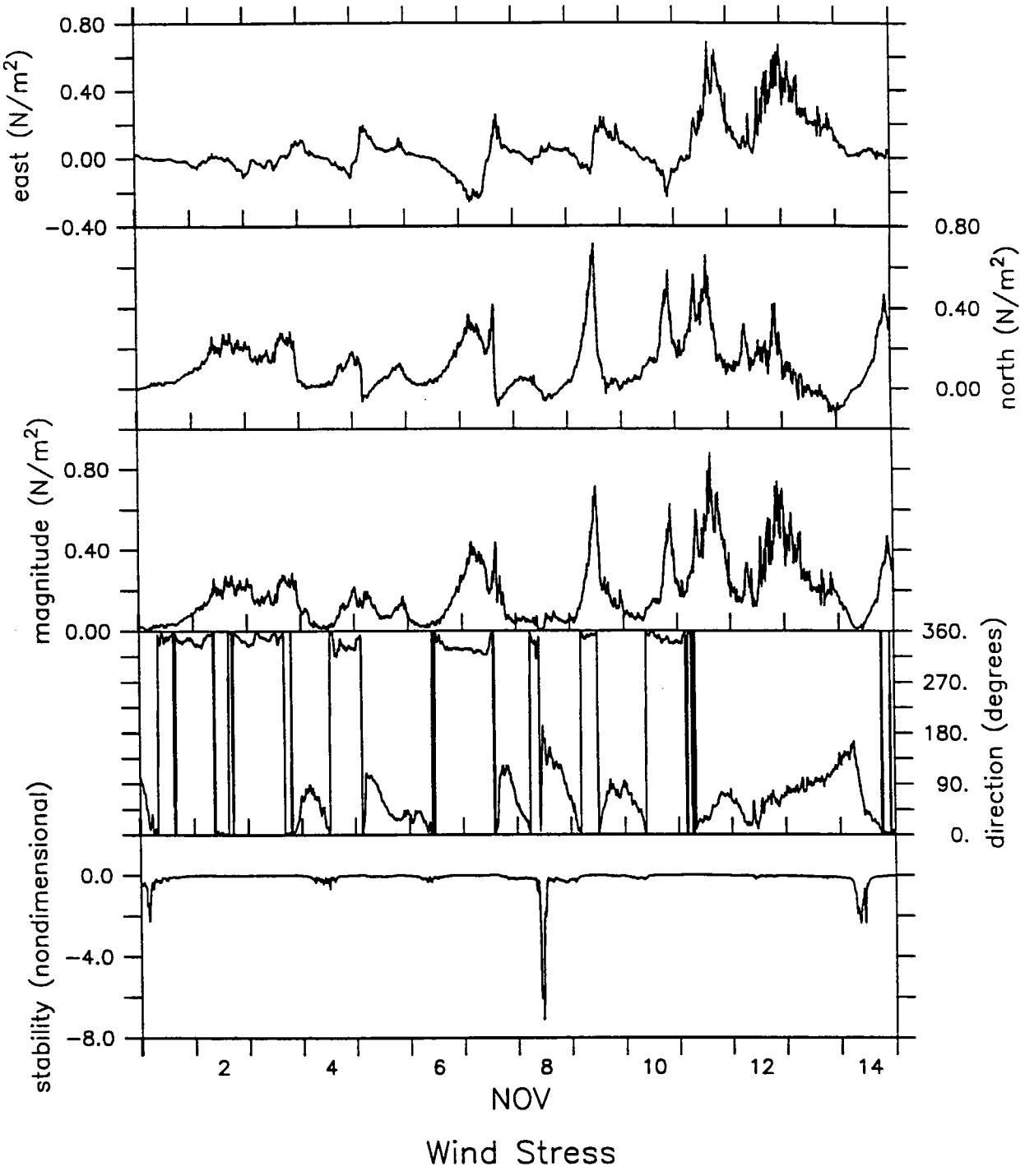

Figure 3.1.11 Wind StressTime Series from VAWR.

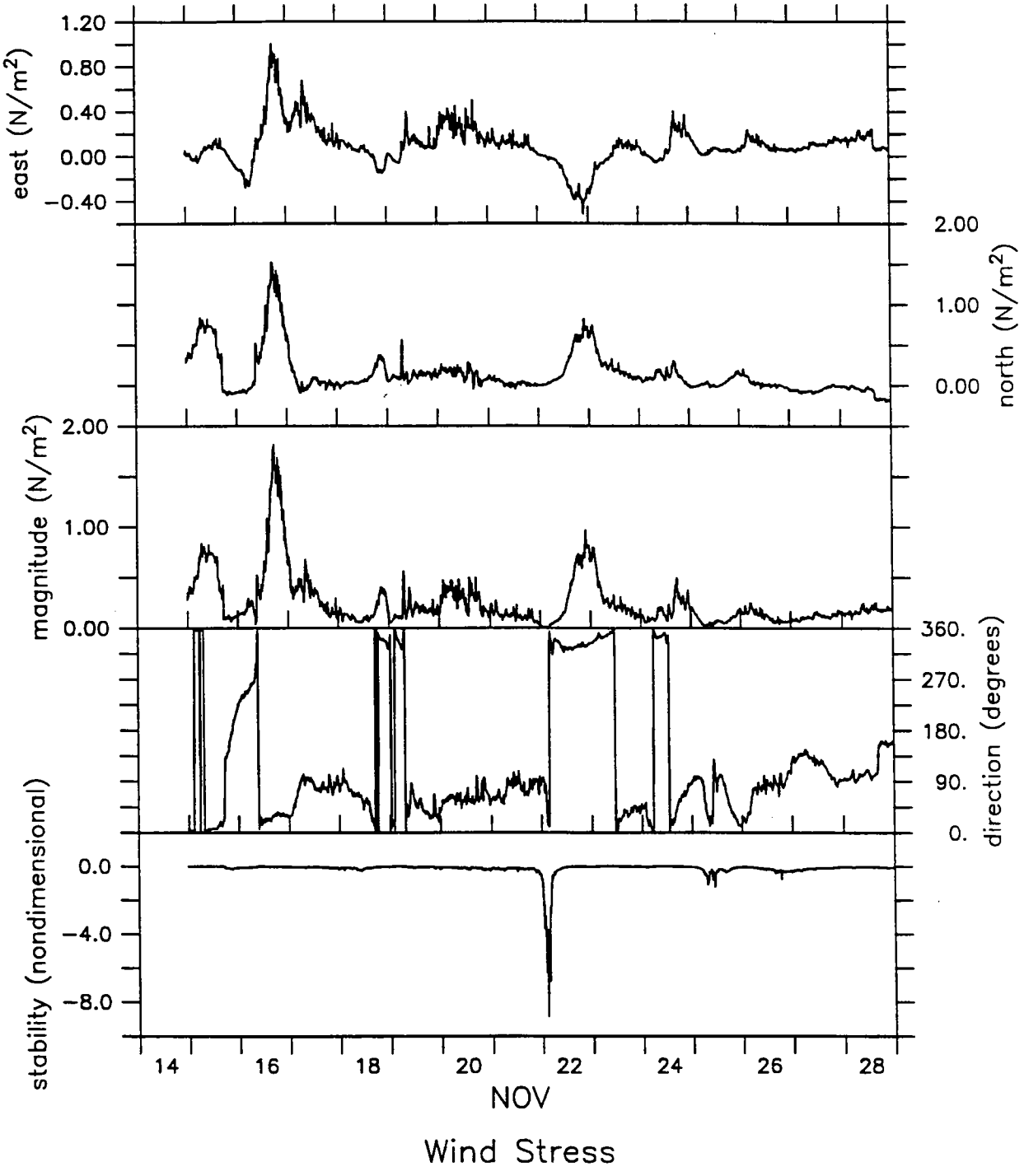

Figure 3.1.12 Wind Stress Time Series from VAWR.

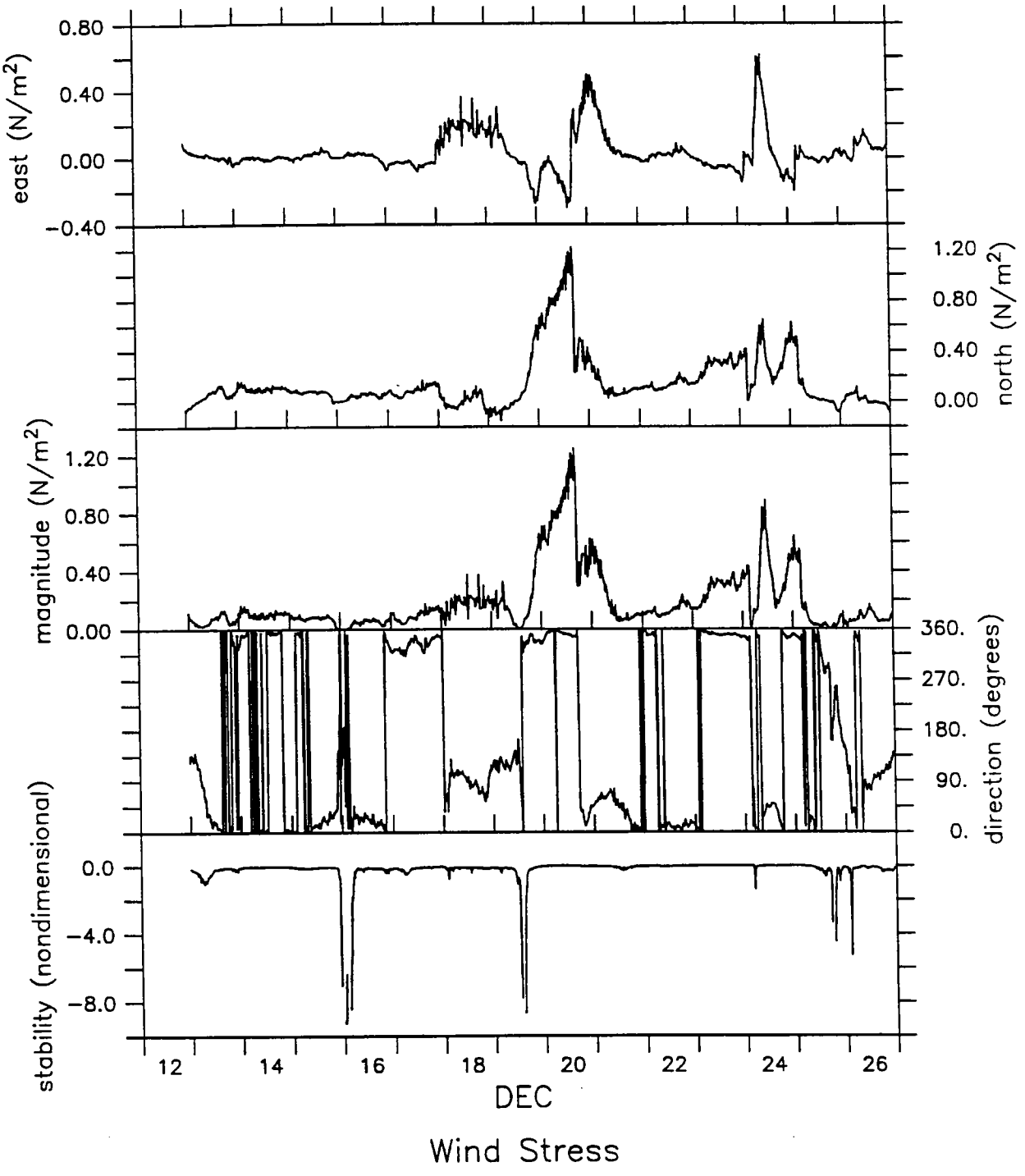

Figure 3.1.13 Wind Stress Time Series from VAWR.

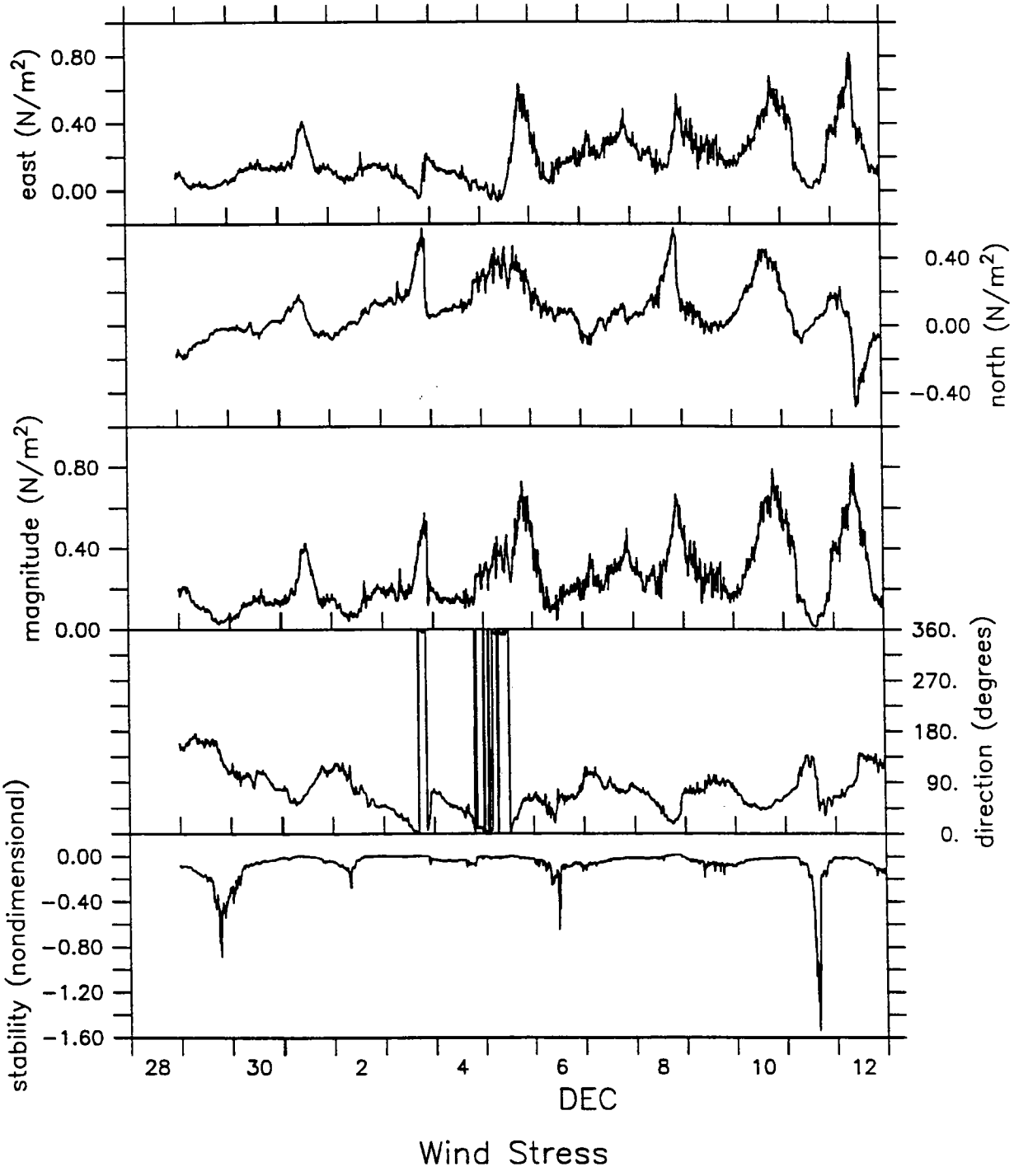

Figure 3.1.14 Wind Stress Time Series from VAWR.

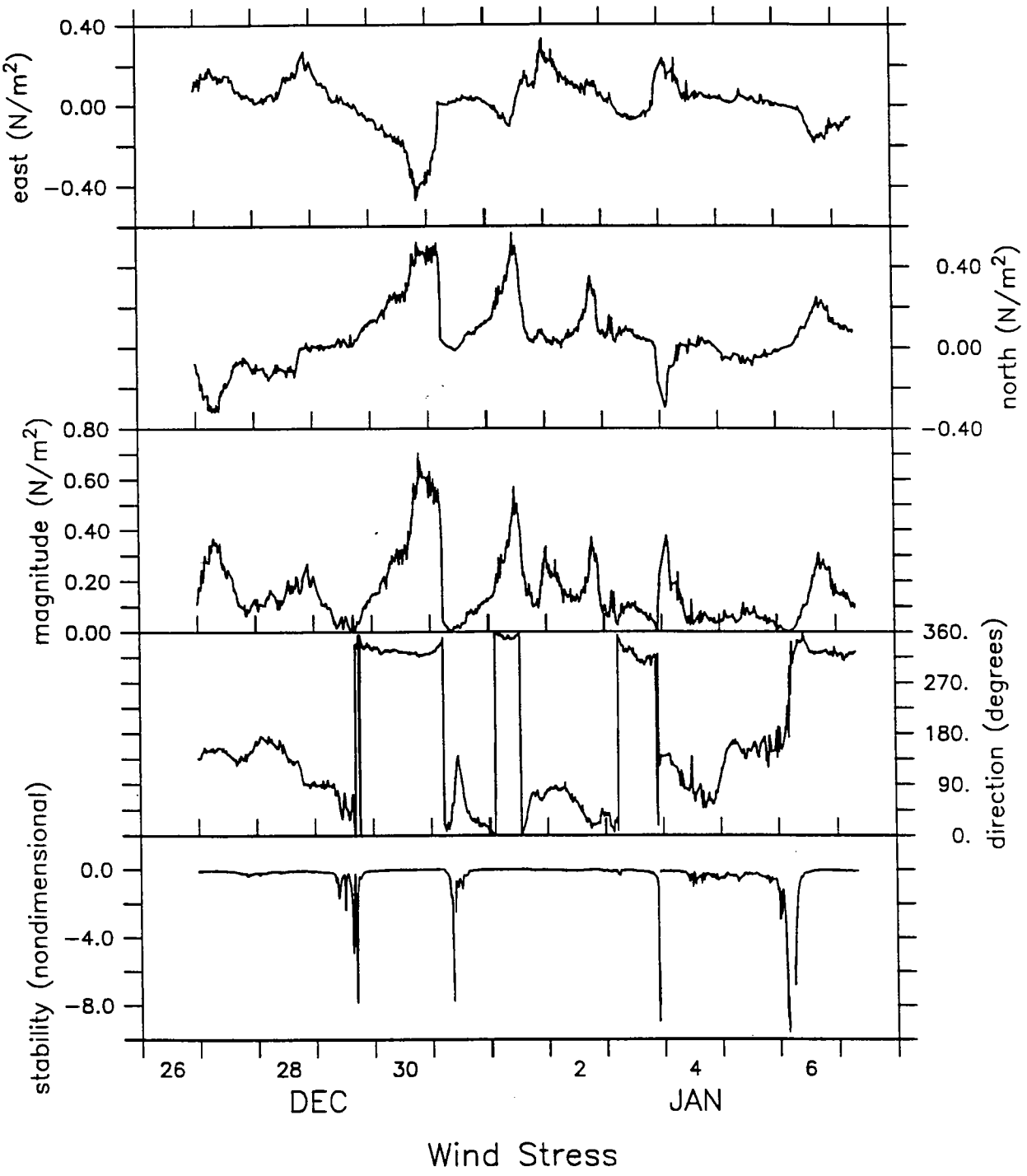

Figure 3.1.15 Wind Stress Time Series from VAWR.

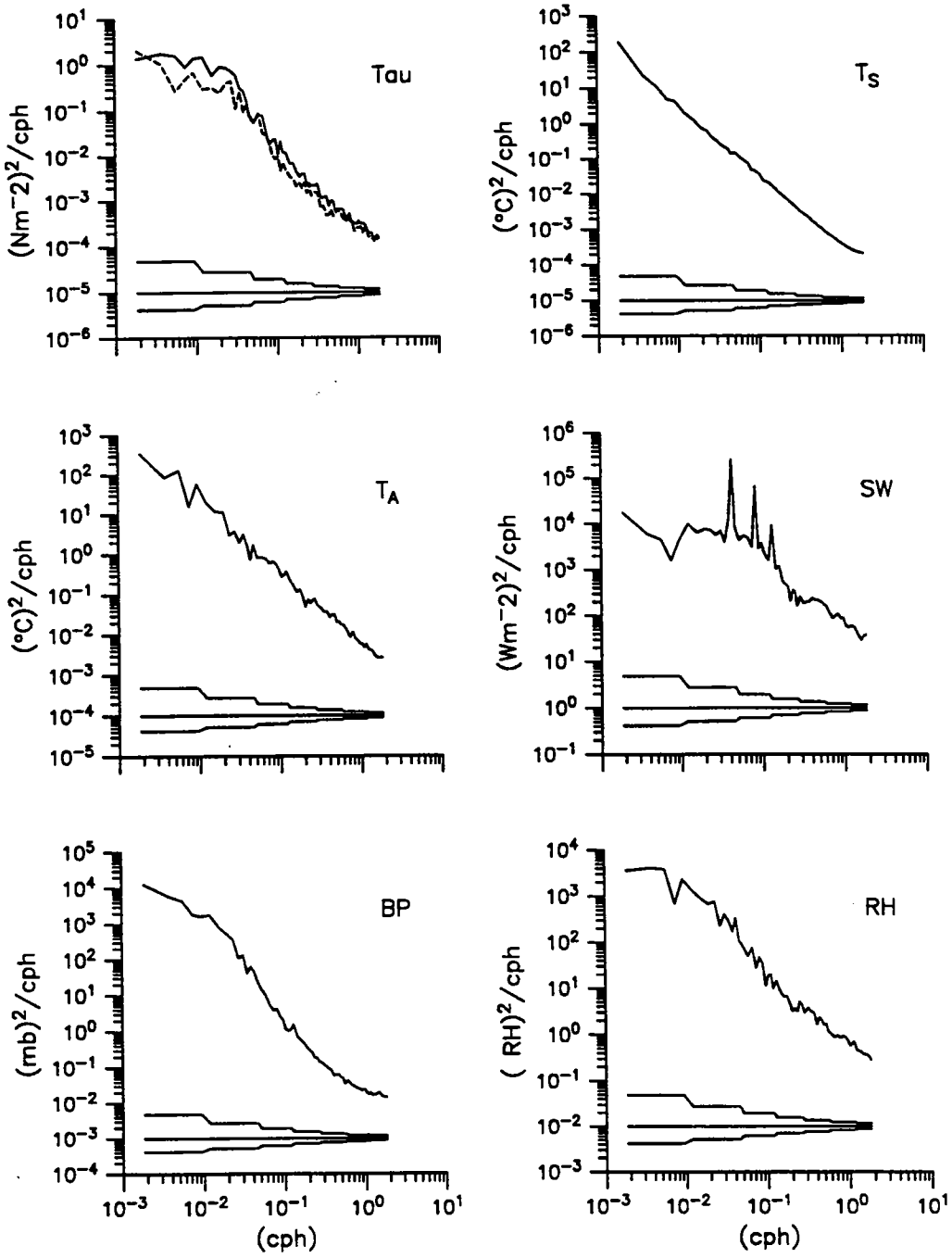

Figure 3.1.16 Autospectra of wind stress, air temperature, barometric pressure, sea surface temperature, insolation, and relative humidity . Rotary autospectra are shown for wind stress; solid curves show the clockwise component, and dashed curves show the counter-clockwise component.

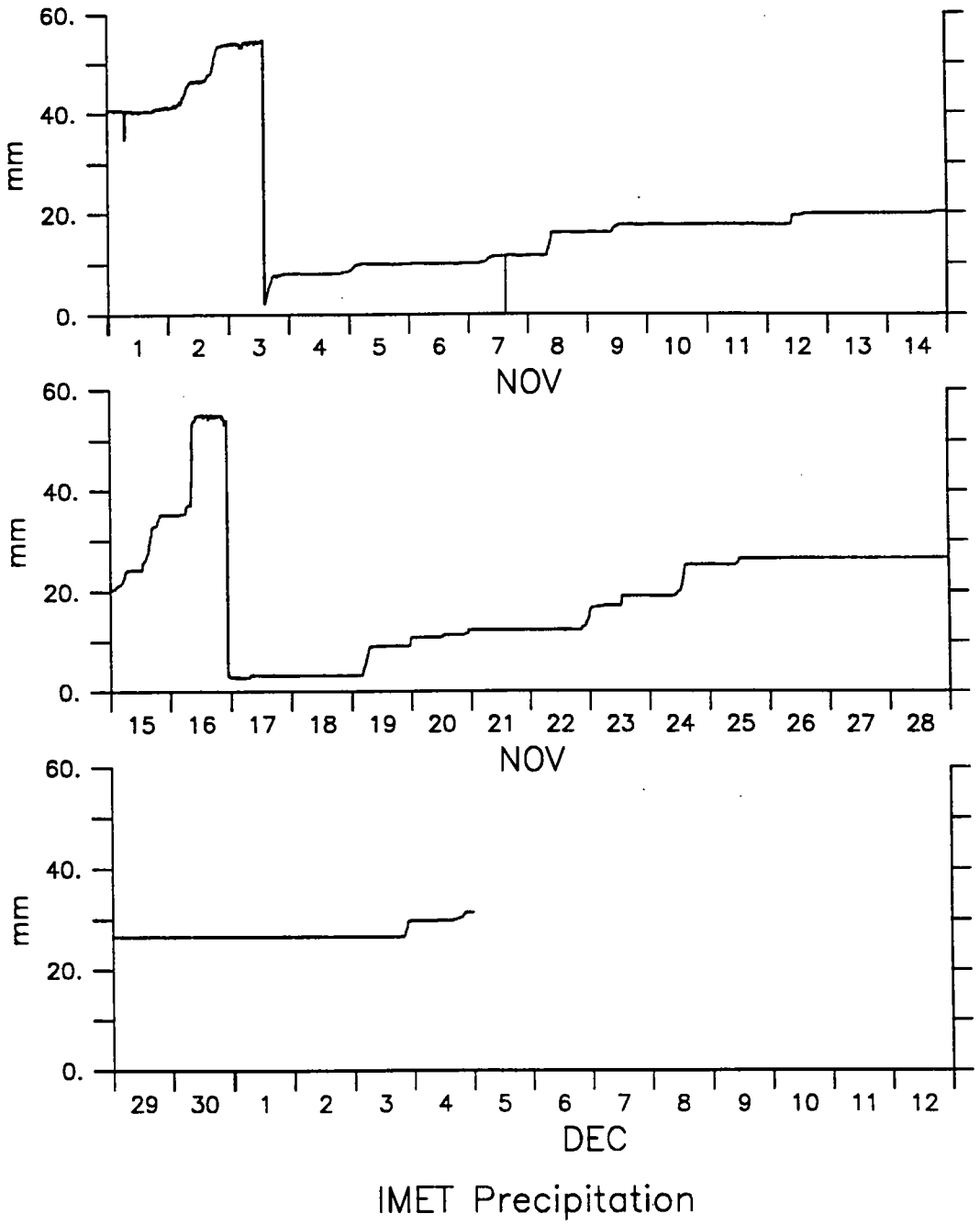

Figure 3.1.17 Cumulative Precipitation in mm measured by IMET system using an R.M. Young self siphoning rain gauge. Rain gauge drains when level reaches a critical value.

3. 2 Temperature and Density Structure during ASREX 91

Sea temperatures were measured by the VAWR, by six Brancker temperature recorders (TPODs) at depths of 2, 40, 60, 80, 100, and 120 meters, and by four Vector Measuring Current Meters (VMCMs) at 5, 10, 15, and 20 meters. VMCMs recorded data every 112.5 seconds, and TPODs recorded every 450 seconds.

Each temperature sensor was calibrated in the lab before and after the experiment, with the exception of TPOD 3700, which did not recieve a post-cruise calibration. Because data comparisons for the shallow instruments looked good using pre-cruise calibrations, all but Brancker 3662, at 60m, were processed with pre-cruise calibrations.

Figure 3.2.1 is a contour plot of all the temperature data from the moored array instruments. Data was filtered using a 24-hour running mean to remove the semidiurnal tide signal, and subsampled at 900 second intervals to produce a uniform time-series for the contour plot.

Time-series and spectra of temperature at each depth are presented in figures 3.2.2 through 3.2.11. In the upper frame of each of these plots, temperature is represented along the y axis and time (UTC) along the x axis. The lower frame contains the spectra. The long arrows on the lower frames indicate the frequency of the semidiurnal tidal peak and the short arrows show the frequency of the Coriolis peak. Confidence limits are displayed at the bottom of the frame. Captions indicate instrument type and depth. Unlike the previous plot,

the data here is not smoothed, so that the strong signals associated with the semidiurnal tides are readily visible.

CTD casts were taken to a depth of about 375 meters. Five casts were taken before deployment of the moored array, and two casts were taken after recovery. Information on CTD cast dates and locations is contained in Appendix 3. Profiles of CTD temperature, salinity, and density are shown in figures 3.2.12 through 3.2.17. These plots show that over the course of the deployment, the mixed layer depth increased from about 40 meters to about 80 meters as indicated by the temperature data alone.

The temperature records in the upper 40 meters of the water column show relatively little short-time variability. The temperature records at 60, 80, 100 and 120 meters show strong peaks at the frequency of the semidiurnal tide. The tidal signal appears to be strongest near the top of the main thermocline.